

Nanofluid Squeezed Flow between Two Riga Plates

Prof. Shivaraya.K
Asst Professor
Dept of Mathematics
Govt First Grade College – Sagara
Shivamogga (dt)

Abstract:

The fundamental concern is to investigate an electro-magneto hydrodynamic (EMHD) pressing progression of half and half nanofluid between stretchable parallel Riga plates. The advantages of the utilization of half and half nanofluids, and the parameters related to it, have been investigated numerically. This specific issue has a great deal of significance in a few parts of building and industry. Warmth and mass exchange alongside nonlinear warm radiation and compound response impacts have additionally been consolidated while completing the investigation. A fitting determination of dimensionless factors have empowered us to build up a scientific model for the present stream circumstance. The subsequent scientific technique have been understood by a numerical plan named as the strategy for minute. The exactness of the plan has been guaranteed by contrasting the present outcome with some officially existing consequences of a similar issue, yet for a restricted case. To back our outcomes further we have likewise acquired the arrangement by another formula strategy joined with the shooting procedure. The mistake examination in an arranged structure have likewise been displayed to approve the gained outcomes. Besides, with the graphical help, the variety in the conduct of the speed, temperature and focus profile have been assessed under the activity of different imbued parameters. The articulations for skin grating coefficient, nearby Nusselt number and neighborhood Sherwood number, if there should arise an occurrence of (Ag – Fe304/H2O) half and half nanofluid, have been determined and the impact of different parameters have additionally been talked about.

Keywords: hybrid nanofluid; nonlinear thermal radiation; heat transfer; chemical reaction; mass transfer; method of moment; numerical results

1. Introduction

An exceptional and amazing advancement in the field of microfluidics, microelectronics, optical gadgets, concoction combination, transportation, high power motors and microsystems, including mechanical and electrical parts, changes the underpinnings of human life. These extensions further interest effective cooling systems, so as to deal with the warm presentation, dependability and long haul operational gadgets. The crude warm administration systems (like cooling through fluids) appear to be lacking, so as to address the difficulties of warm proficiency. Later on, this issue has been settled by scattering nano-meter estimated structures, inside the host liquid, which positively impacts its thermo-mechanical properties. In such manner, Choi [1,2] was considered as the pioneer, who gave this idea and calls it 'Nanofluid'. Numerous analysts have proposed different hypothetical models for warm conductivity, by following his strides. Maxwell [3] took a shot at a model for the warm conductivity which is reasonable just for the circular molded nanoparticles. Further investigations around there lead us to an assortment of models, containing the effect of, molecule associations (i.e., Bruggeman model, 1935) [4], particles shapes (i.e., Hamilton and crosser model 1962) [5] and particles appropriation (i.e., Suzuki et al. 1969) [6]. Besides, specialists have discovered various articles in the writing that covers the various parts of the nanofluid. Some of them can be found in the references [7–12].

In later past years, another class of nanofluids, entitled "Half and half nanofluid", have appeared that bears high warm conductivity when contrasted with that of mono nanofluid. They have acquired an insurgency different warmth move applications like atomic framework cooling, generator cooling, electronic cooling, vehicle radiators, coolant in machining, oil, welding, sunlight based warming, warm capacity, warming and cooling in structures, biomedical, tranquilize decrease, refrigeration, and barrier and so on. On account of a standard nanofluid, the basic issue is it is possible that they have a decent warm conductive system or show a superior rheological properties. The nanocomposites (without any assistance) don't have all the potential highlights which are required for a specific application. In this manner, by a fitting choice of at least two nanoparticles, half breed nanofluid can lead us to a homogeneous blend, which has every physicochemical property of different substances that can barely be found in an individual substance [13,14].

The unmistakable highlights of half and half nanofluid have picked up the consideration of overall scientists and along these lines various research articles have been distributed in the course of recent years. By utilizing another material structure idea, Niihara [15] talked about that the mechanical and warm properties of the host liquid can be significantly upgraded, by the incorporation of nanocomposites. Jana et al. [16] inspected the warm proficiency of the host liquid, by joining single and half and half nanoparticles. Suresh et al. [17] considers a two-advance technique so as to incorporate water-based (Al₂O₃ – Cu) half breed nanofluid. Their exploratory outcomes uncover an improvement in the consistency and warm properties of the readied cross breed nanofluid. In their next examination [18], the impacts of (Al₂O₃ – Cu) half and half nanofluid on the rate of warmth move have been researched. Momin [19], in 2013, led an examination to think about the effect of blended convection on the laminar progression of half and half nanofluid inside a slanted cylinder. By utilizing a numerical plan, Devi and Devi [20] explored the impact of magneto hydrodynamic progression of H₂O based (Cu – Al₂O₃) crossover nanofluid, over a permeable widening surface. With the guide of entropy age, the magneto hydrodynamic progression of water based (Cu – Al₂O₃) half and half nanofluid, inside a penetrable channel, has been talked about by Das et al. [21]. Chamkha et al. [22], numerically dissected, the time ward conjugate regular convection of water based half and half nanofluid, inside a crescent depression The Blasius stream of cross breed nanofluid with water, taken as a base liquid over a convectively warmed surface, has been inspected by Olatundun and Makinde [23]. Moreover, in [24], Hayat and Nadeem consolidated the silver (Ag) and copper oxide (CuO) as nanoparticles inside the water, to improve the rate of warmth move, over the directly extending surface.

Nowadays, analysts have been pulled in, to break down the pressing streams in different geometries. Because of their centrality, they have been associated with numerous useful and modern circumstances, as biomechanics, sustenance handling, and substance and mechanical designing. They have additionally been used, so as to look at the arrangement of grease, polymer preparing, car motors, orientation, infusion, gear, apparatuses and so on. These stream marvels have been seen in various hydro dynamical machines and gadgets, where the ordinary speeds are upheld by the moving dividers of the channel. Stefan [25] was the pioneer behind this idea. Later on, Shahmohamadi et al. [26] utilized a logical method, to look at the time-subordinate

axisymmetric stream of a crushed sort. As of late, the impacts of crushing stream on nanofluid, restricted between parallel plates, have been researched by M. Sheikholeslami et al. [27]. They likewise used the Adomian's disintegration technique to discover the arrangement of the individual stream model. Khan et al. [28] have considered, the gooey dispersal impacts alongside slip condition, to dissect the two-dimensional crushing progression of copper-water based nanofluid. For arrangement strategy, they have utilized a variety of the parameters technique. In 2017, the crushing consequences for the magneto hydrodynamic progression of Casson liquid (inside a channel) have been completely investigated by Ahmed et al. [29]. They have displayed the separate stream issue and after that settled it both numerically (Runge-Kutta plan of fourth request) and logically (Variety of parameters technique).

Gallites and Lilausis [30] thought of the possibility of an electromagnetic actuator gadget, so as to set up the crossed attractive and electric fields, that properly incited the divider's parallel Lorentz powers. The motivation behind that gadget was to control the stream attributes, which for the most part have a range shrewd course of action of rotating and constant magnets that explicitly mounted a plane surface. The gadget, here and there showed as Riga plate [31], gave a guide to diminish the weight drag, just as the rubbing of submarines, that can be accomplished by lessening the choppiness generation and a limit layer division. Various research articles have been distributed, so as to investigate the unmistakable highlights of the laminar progression of a liquid because of Riga plate. By expecting the least electrical conductivity impacts, Pantokratoras and Magyari [32] explored the stream conduct alongside free convection. In 2011, Pantokratoras [33] announced the exhibition of Blasius stream, implemented by the Riga plate. He likewise encountered the Sakiadis stream in his examination. Later on, Magyari and Pantokratoras [34] considered the Blasius stream of the fluid, which in the meantime is electrically leading, actuated by Riga surface. The electro magneto hydrodynamic progression of nanofluid, initiated by Riga plate alongside the slip outcomes, have been analyzed by Ayub et al.[35]. In 2017, Hayat et al. [36], talked about the crushing progression of a liquid between two parallel Riga plates, together with convective warmth move. The warm radiative impacts joined by synthetic response, were additionally a piece of their examination. Also, Hayat et al. [37] examined the electro magneto crushing progression of carbon nanotube's suspended nanofluid between two parallel rotatory Riga plates alongside thick dissemination impacts. They have considered the softening warmth move condition, which essentially uncovered that the warmth directing procedure to the strong surface, included the join impacts of both reasonable and dissolving heat, which fundamentally upgrades the temperature of the strong surface to its liquefying temperature.

The warm radiation is a critical method of warmth move [38,39], which is by all accounts overwhelming, so as to move the net measure of warmth, even in the presence of free or constrained convection. The exchange of warmth by means of radiation have been altogether found in many designing and modern applications, including planes, space vehicles, satellites, and nuclear power plant. In this specific situation, numerous scientists have completely talked about the radiative warmth move

wonders. Probably the most significant have been found in [40–44].

The writing study uncovered the way that no single step has been taken so as to examine the notable highlights of (Ag – Fe304H20) crossover nanofluid, between two parallel Riga plates. This article experiences the persuasive conduct of the viscid progression of (Ag – Fe304H20) crossover nanofluid between two parallel Riga plates, where the lower plate encounters an extending speed, while the upper plate upholds a crushing stream. The exchange of warmth and mass alongside nonlinear warm radiative and compound response impacts would likewise be a piece of this examination. By utilizing the appropriate comparability changes, a scientific model for the present stream circumstance have been cultivated. Technique for minute alongside Runge-Kutta-Fehlberg strategy have been considered to discover the arrangement of the model. Tables have been given which displays the legitimacy of the gained outcomes. Besides, the graphical guide has been given, to exhibit the impact of different instilled substances, on the speed and temperature alongside fixation profiles. The articulations identified with the coefficient of skin grinding, nearby Nusselt number and neighborhood Sherwood number have additionally been created

2. Formulation of the Governing Equations

Two parallel Riga plates have been under consideration, among which an electro-magneto hydrodynamic (EMHD) flow of (Ag – Fe₃O₄/H₂O) hybrid nanofluid has been flowing. The flow is also time dependent and incompressible. Cartesian coordinates have been chosen in such away, that the \check{x} –axis coincides with the horizontal direction, whereas the \check{y} –axis is placed normal to it. The lower plate positioned at $\check{y} = 0$, experiences a stretching velocity $\check{u}_c(\check{x}) = a\check{x}/(1 - h\check{y})$. Besides, the upper Riga plate, owing the place at $\check{y} = P(\check{y}) = \frac{-\beta}{2} (a/u_f (1 - h\check{y}))^{-0.5}$. It is further assumed that the flow of (Ag – Fe₃O₄/H₂O) hybrid nanofluid is a squeezing flow.

3. Results and Discussions

The goal is to graphically elucidate the influential behavior of velocity, temperature and concentration profiles, due to the various ingrained entities. . A pictorial view, from Figure 2 to Figure 20, has been presented for the above-mentioned purpose. Figures 2–4 displays the performance of velocity profile, under the action of the squeezing parameter, Modified Hartmann number and solid volume fraction. The variations in velocity component $\check{F}^u(3)$, due to squeezing parameter y , have been depicted in Figure 2a. For $y > 0$, i.e., when the upper plate moves in the downward direction, the fluid nearby the upper wall experiences a force, which in turn enhances the fluid velocity in that region. As y increases sufficiently, the velocity component $\check{F}^u(3)$ also increases and gradually depreciates the reversal behavior of the flow. The velocity component $\check{F}(3)$ also experiences an increment in the region, adjacent to the upper wall, which is mainly due to the squeezing behavior of the upper plate and this phenomena has been clearly observed through Figure 2b. Figure 3 demonstrates the impact of Modified Hartmann number \mathcal{M}_p on the axial and normal components of the velocity distribution. Since the magnetic field experiences an exponential decline, therefore velocity component $\check{F}^u(3)$ seems to be increased in the lower region of the channel. The fact behind is that the application of magnetic field generates the Lorentz forces, which in turn opposes the fluid flow. But in the present situation, the magnetic field decreases, so the Lorentz forces decreases and consequently, an increment in velocity has been perceived in the region close to the lower Riga plate. Besides, in the upper half, the velocity displays an opposite behavior as compared to the lower half

of the channel, which may be due to the downward squeezing motion of the upper plate. Figure 3b exhibits an increment in the normal component of velocity $\check{F}(3)$ with the increasing Modified Hartmann number, which is primarily be due to the decreasing effects of Lorentz force. It can be detected from Figure 4a that the axial velocity decreases in the lower region with the increasing nanoparticles concentration, while an opposite behavior has been perceived in the upper portion of the channel. The reason behind is that the nanoparticle’s concentration resists the fluid to move and therefore decreases the fluid velocity. Figure 4b depicts a decline in the normal component of the velocity $\check{F}(3)$ with increasing nanoparticle’s concentration, which opposes the fluid motion. Moreover, the inset pictures reveal the fact that the velocity for the (Fe₃O₄/H₂O) nanofluid mostly attains the higher values as compared to the (Ag – Fe₃O₄/H₂O) hybrid nanofluid.

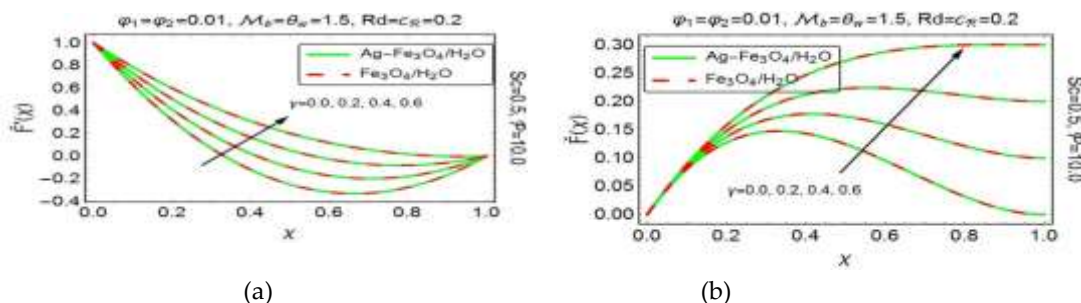


Figure 2. Impact of particular values of y on (a) $\check{F}^u(3)$ and (b) $\check{F}(3)$.

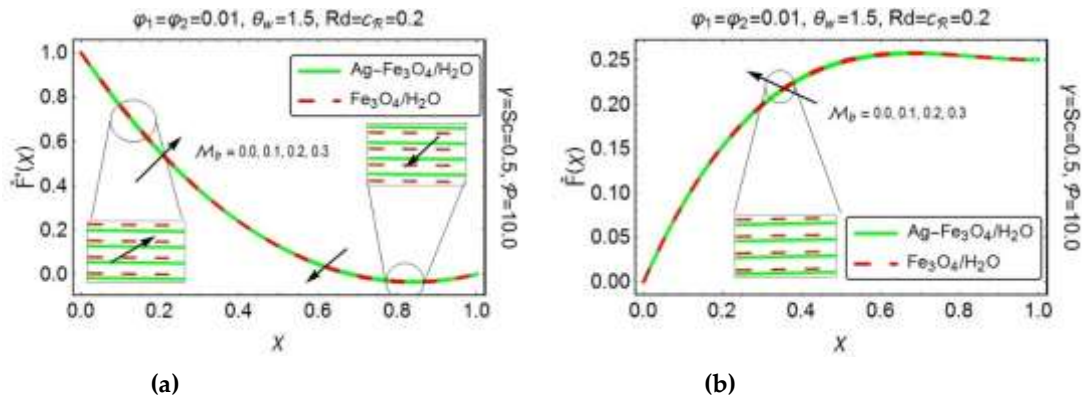


Figure 3. Impact of particular values of M_p on (a) $\check{F}''(3)$ and (b) $\check{F}'(3)$.

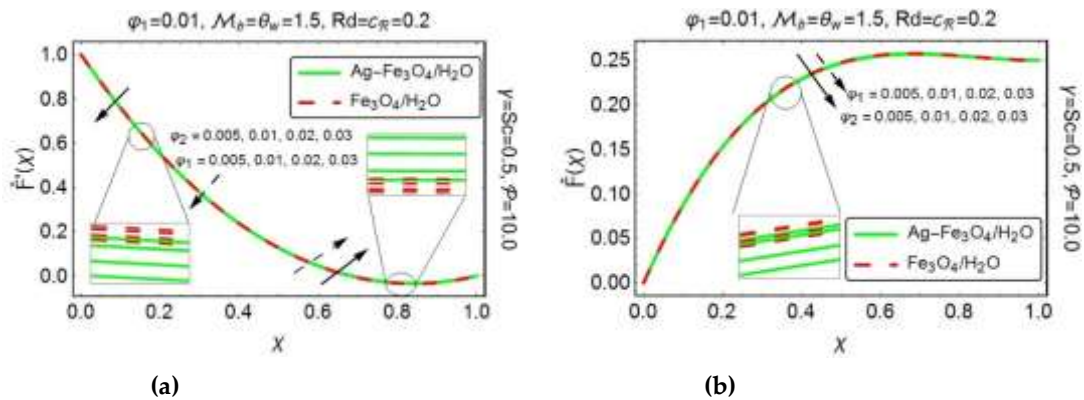


Figure 4. Impact of particular values of φ_1 and φ_2 on (a) $\check{F}''(3)$ and (b) $\check{F}'(3)$.

The upcoming figures give a pictorial description of the variations in temperature distribution, for various embedded parameters. Figure 5 displays the impact of squeezing parameter γ on temperature profile. When the upper plate squeezed down, i.e., $\gamma > 0$, it exerts a force on the nearby fluid and enhances its velocity, but since the temperature seems to be dominant at the lower wall therefore the fluid in the adjacent region experiences the higher temperature values as compared to the region nearby the channel's upper wall. To demonstrate the impact of Modified Hartmann number M_p on temperature distribution, Figure 6 has been plotted. It has been found that temperature reveals lower values, as M_p increases. As the impact of Lorentz force on velocity profile produce a friction on the flow, which mainly be responsible to produce more heat energy. In the present flow situation, since the magnetic field exponentially decreases, so the Lorentz force decreases which in turn generates less friction force and consequently, decreases the heat energy and therefore decreases the fluid's temperature as well as the thermal boundary layer thickness. From Figure 7, one can clearly observe an increment in temperature profile with increasing nanoparticles concentration. The fact behind is that, the inclusion of nanoparticles with different volume fractions augments the thermal properties of the host fluid and therefore increases its temperature. It has also been observed that the temperature of (Ag – Fe₃O₄/H₂O) hybrid nanofluid shows its supremacy over the (Fe₃O₄/H₂O) nanofluid, which definitely be due to the rising values of the thermal conductivity for (Ag – Fe₃O₄/H₂O) hybrid nanofluid.

Figure 8 has been sketched, to highlight the temperature behavior under the influence of radiation parameter R_d . An upsurge has been encountered in temperature, for increasing R_d . The fact behind is that, the increasing R_d corresponds to the decrement in mean absorption coefficient, which in turn raises the fluid temperature. The temperature

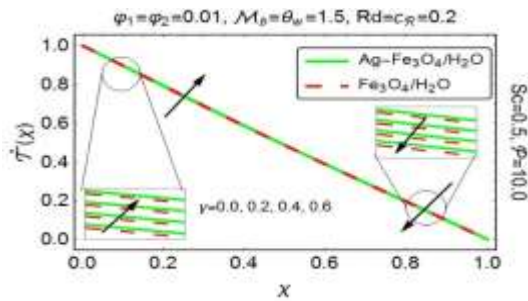


Figure 5. Impact of particular values of y on $\xi(3)$.

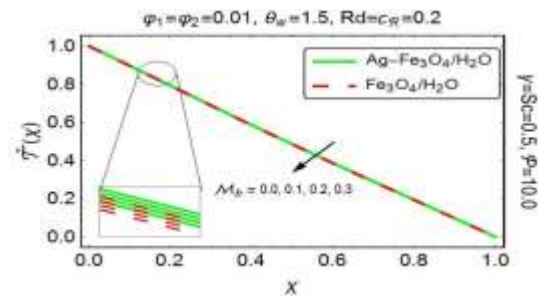


Figure 6. Impact of particular values of ϕ on $\xi(3)$.

also depicts a rising behavior with increasing $8c$ (see Figure 9). The increasing $8c$ implies that the temperature differences between the lower and upper walls significantly rises and subsequently, an increment in temperature has been recorded.

on $\xi(3)$.

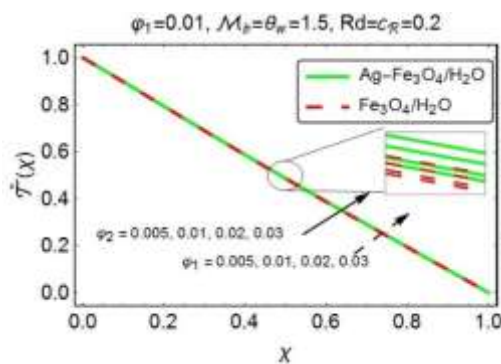


Figure 7. Impact of particular values of ϕ_1 and ϕ_2 on $\xi(3)$.

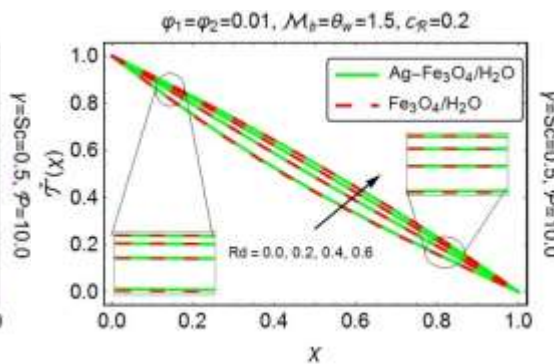


Figure 8. Impact of particular values of R_d on $\xi(3)$.

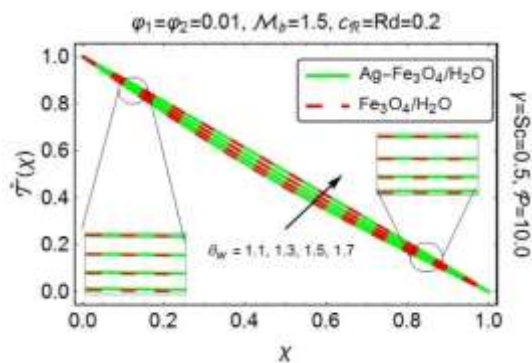


Figure 9. Impact of particular values of $8c$ on $\xi(3)$.

The next set of figures provide us an aid, to visualize the deviations, in concentration profile, caused by various embedded parameters. Figure 10 demonstrates the influence of squeezing parameter y on the concentration profile. When the upper plate moves vertically downward, i.e., $y > 0$, it suppresses the adjacent fluid layers and enhances its velocity, but since the concentration shows its supremacy at the lower wall, therefore the concentration profile shows its dominance in the region, close to the lower wall, as compared to the region adjacent to the upper wall. To demonstrate

the impact of Modified Hartmann number \mathcal{M}_p on concentration profile, Figure 11 has been painted. As explained earlier that the Lorentz forces, in present flow situation, experience a decline, which as a result generate less friction force and therefore, decrease the concentration profile along with concentration boundary layer thickness. From Figure 12, one can clearly detect a decline in concentration profile, as nanoparticle fraction increases. Moreover, it has been noticed that the concentration profile for (Ag – Fe₃O₄/H₂O) hybrid nanofluid possesses lower values as compared to the (Fe₃O₄/H₂O) nanofluid.

Figure 13 portrays the influence of chemical reaction parameter c_R on concentration profile. A clear decline has been perceived in the concentration of species with the growing values of chemical reaction parameter c_R . Since the chemical reaction, in the present flow analysis, is due to the consumption of the chemicals, therefore, the concentration profile experiences a decline with the increasing values of c_R . The variations in concentration profile, under the action of Schmidt number Sc, has been presented in Figure 14. It has been observed that the increasing values of Schmidt number Sc causes a decline in the concentration of the species. Since the Schmidt number is the ratio

of momentum diffusivity to mass diffusivity. Therefore, the increment in Schmidt number consequently implies a decline in mass diffusivity, which in turn decreases the concentration profile.

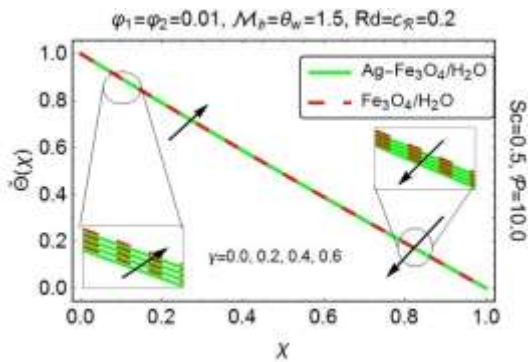


Figure 10. Impact of particular values of y on $\theta(3)$

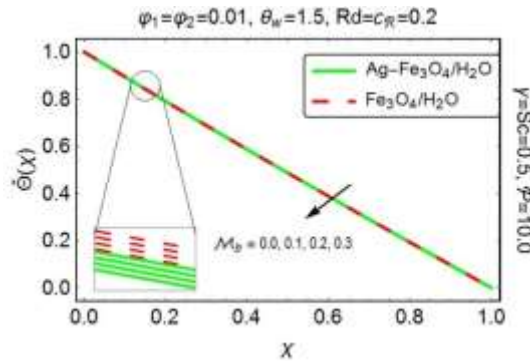


Figure 11. Impact of particular values of \mathcal{M}_p on $\theta(3)$.

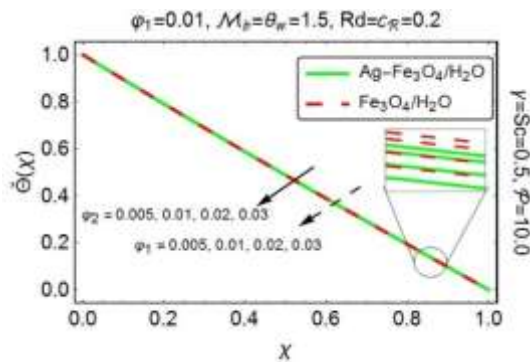


Figure 12. Impact of particular values of ϕ_1 and ϕ_2 on $\theta(3)$.

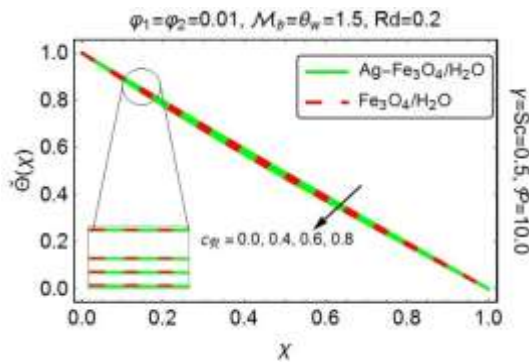


Figure 13. Impact of particular values of c_R on $\theta(3)$.

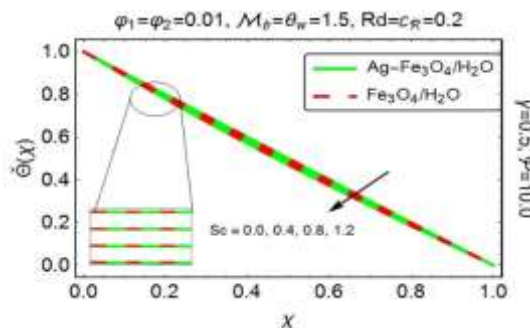


Figure 14. Impact of particular values of Sc

on $\delta(3)$.

Figures 15 and 16 display the impact of various ingrained parameters on the skin friction coefficient, both at the upper and lower Riga surfaces. It has been detected from Figure 15 that increasing the nanoparticles concentration certainly enhances the coefficient of skin friction drag at the lower Riga plate. However, at the upper plate, an opposite behavior has been clearly visible. As far as squeezing parameter γ is concerned, the skin friction coefficient exhibits an increasing behavior, in the region adjacent to the lower plate. However, a decline has been perceived at the

upper wall. From Figure 16, one can clearly observe an increment in skin friction coefficient, with the increasing M_p , both at the upper and lower Riga plates. Moreover, the skin friction coefficient for (Ag – Fe₃O₄/H₂O) hybrid nanofluid possesses higher values, at the bottom of the channel, as compared to the (Fe₃O₄/H₂O) nanofluid.

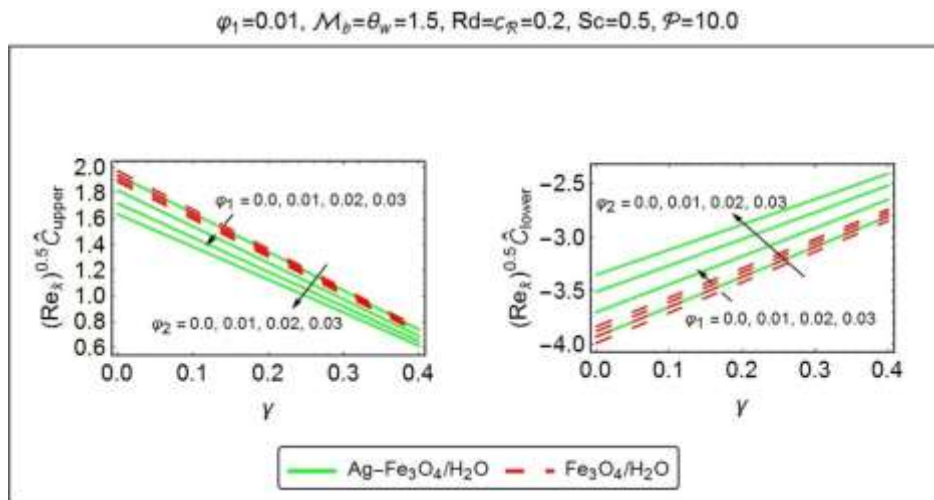


Figure 15. Coefficient of skin friction drag for particular values of ϕ_1 and ϕ_2 .

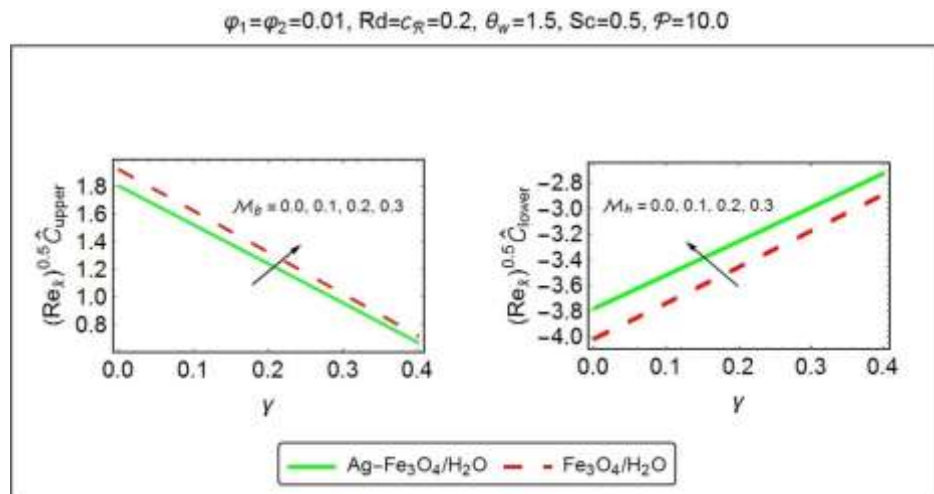


Figure 16. Coefficient of skin friction drag for particular values of M_p .

Figures 17 and 18 have been plotted, to assess the consequences of various embedded entities on the local rate of heat transfer i.e., Nusselt number. From Figure 17, one can clearly detect an increment in heat transfer, with increasing nanoparticle volume fraction, at both of the plates. Since the nanoparticle’s inclusion, in the base fluid, is responsible for rising its temperature, therefore an augmentation in the heat transfer rate is quite obvious. By varying the squeezing number γ horizontally, the local Nusselt number at the upper as well as on the lower plates, indicate a decreasing behavior. Figure 18 depicts the variations in heat transfer rate, with growing values of radiation parameter R_d and temperature difference parameter θ_c . Since both the parameters (R_d and θ_c) significantly amplifies the temperature of the fluid, therefore, they play a key role in enhancing the local Nusselt number, both at the upper and lower Riga plates. Besides, it has been observed from both the figures that the (Ag – Fe₃O₄/H₂O) hybrid nanofluid shows its supremacy in transferring the heat, both at the upper and lower Riga plates.

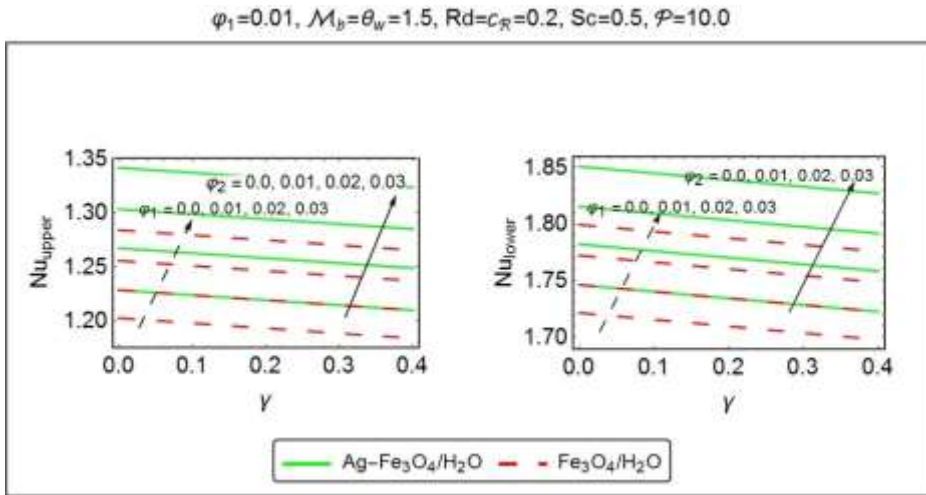


Figure 17. Local Nusselt number for particular values of ϕ_1 and ϕ_2 .

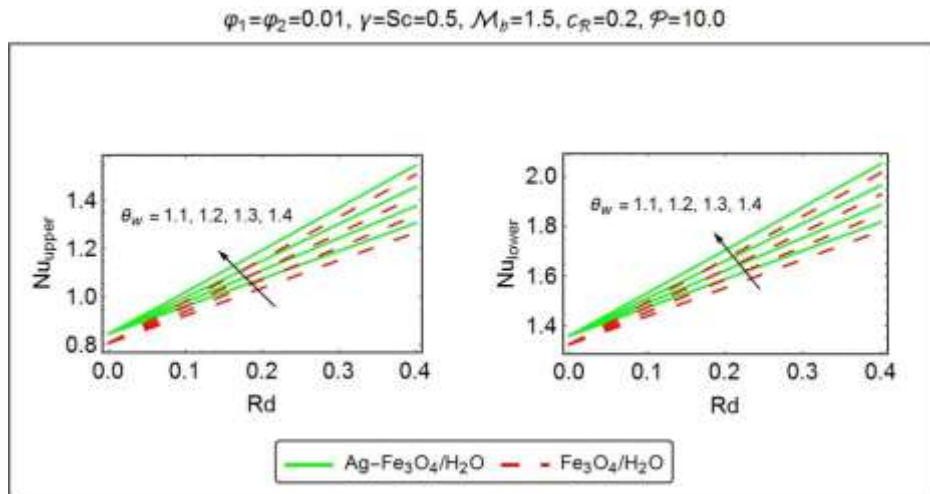


Figure 18. Local Nusselt number for particular values of θ_w .

Figures 19 and 20 depict the variations in the rate of mass transfer, i.e., Sherwood number under the action of various involved parameters. Figure 19 reveals a decline in the Sherwood number with increasing nanoparticle concentration, both at the upper and lower Riga plates. Since the increasing nanoparticle's volume fraction certainly opposes the fluid motion, therefore a decrement in Sherwood number is quite obvious. The rate, with which mass flows, also shows a decreasing behavior when the squeezing parameter γ increases horizontally. From Figure 20, one can observe a clear enhancement in the rate of mass flow in the region nearby the lower plate, when the chemical reaction parameter c_R increases curve wise and Schmidt number Sc varies along the horizontal axis. On the other hand, a reverse behavior has been perceived at the upper plate. Moreover, (Fe_3O_4/H_2O) nanofluid remains dominant in transferring the mass, both at the upper and lower Riga plates.

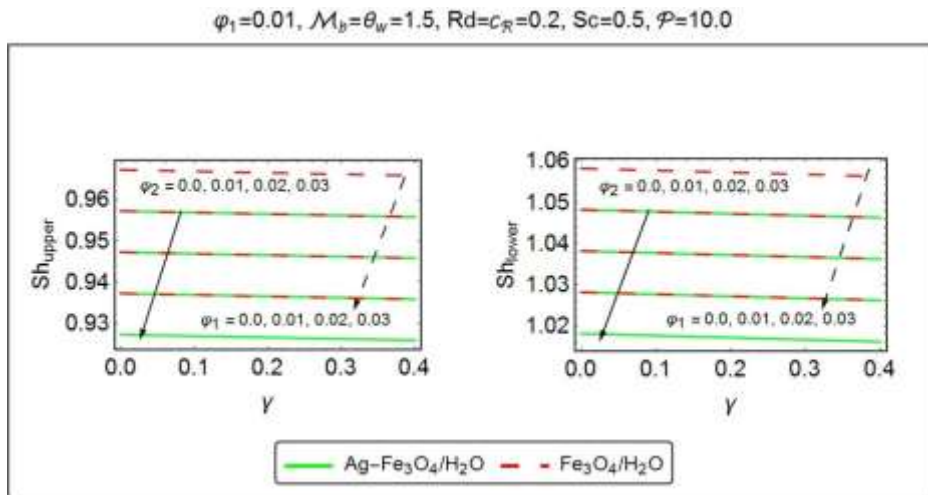


Figure 19. Sherwood number for particular values of ϕ_1 and ϕ_2 .

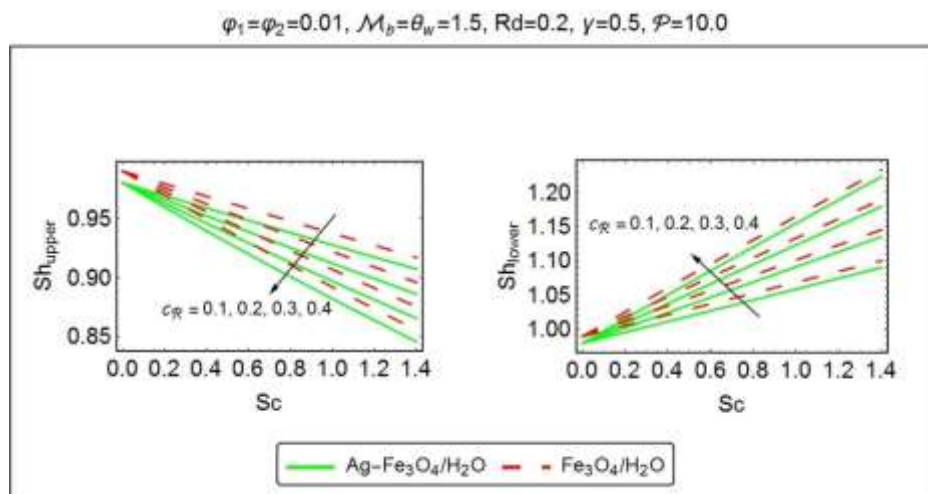


Figure 20. Sherwood number for particular values of c_R .

Hybrid nanofluids, being advanced version of nanofluids, considerably influences the thermo- mechanical properties of the working fluid, particularly the thermal conductivity. For the said purpose, Tables 6 and 7 have been designed, to see the deviations in thermo-mechanical properties of the (Ag – Fe₃O₄/H₂O) hybrid nanofluid and (Fe₃O₄/H₂O) nanofluid. It has been detected that the density of (Ag – Fe₃O₄/H₂O) hybrid nanofluid depicts an increment, as compared to (Fe₃O₄/H₂O) nanofluid. While, the specific heat clearly experiences a decline with the increasing nanoparticles fraction. As far as thermal conductivity is concerned, (Ag – Fe₃O₄/H₂O) hybrid nanofluid shows a dominant behavior against the (Fe₃O₄/H₂O) nanofluid. Besides, the Bruggeman model (18), for thermal conductivity shows its proficiency over the Maxwell’s model (17). The reason is that, the Bruggeman model is more focused on the maximum interactions between randomly dispersed particles. It usually involves the spherical shaped particles, with no limitation on the particles concentration. On the other hand, the Maxwell’s model depends on the nanoparticle’s volume fraction and the thermal conductivity of the base fluid and the spherical shaped particles.

Table 6. Variation in thermo-physical properties of (Ag – Fe₃O₄/H₂O) hybrid nanofluid with ($\gamma = 0.01$).

γ	$\check{\eta}$	$\check{\eta}C_p \times 10^6$	$A_{Mn\uparrow}$ (14)	$A_{Mn\uparrow}$ (13)
0.00	1038.929	4.159918091	0.628640157	0.628422974
0.02	1228.987	4.125930473	0.67317743	0.6695051201
0.04	1419.045	4.091942855	0.72042306	0.7092486827
0.06	1609.103	4.057955237	0.77474778	0.7506805172
0.08	1799.161	4.023967619	0.83787931	0.7939214931
0.10	1989.219	3.989980001	0.91213707	0.8390950667

Table 7. Variation in Thermo-physical properties of (Fe₃O₄/H₂O) nanofluid with ($\gamma = 0$).

γ	$\check{\eta}$	$\check{\eta}C_p \times 10^6$	$A_{n\uparrow}$ (14)	$A_{n\uparrow}$ (13)
0.00	997.1	4.1668809	0.613	0.613
0.02	1080.758	4.152955282	0.644998753	0.6441068291
0.04	1164.416	4.139029664	0.680047429	0.6762841143
0.06	1248.074	4.125104046	0.718527614	0.7095880769
0.08	1331.732	4.111178428	0.760870799	0.7440789486
0.10	1415.39	4.09725281	0.80756218	0.779821329

4. Conclusions

This article discloses the salient features of nonlinear thermal radiation, in the squeezing flow of (Ag – Fe₃O₄/H₂O) hybrid nanofluid, between two Riga plates along with a chemical reaction. Method of moment has been employed for the solution point of view. The obtained results are then compared with the numerical results (obtained via Runge-Kutta-Fehlberg algorithm). Both the methods depict an excellent agreement between the results.

Further investigations are as follows:

- Velocity profile seems to be an increasing function of both squeezing parameter γ and modified Hartmann number \mathcal{M}_p .
- A decrement in the velocity behavior has been perceived, with increasing nanoparticle concentration.
- The velocity profile for (Ag – Fe₃O₄/H₂O) hybrid nanofluid mostly remains on the lower side.
- The amplification in temperature has been recorded for increasing squeezed number γ and nanoparticle concentration, while a reversed behavior has been noticed for increasing modified Hartman number \mathcal{M}_p .
- The temperature behaves in an increasing manner with the rising Rd and θ_c . Besides, the temperature profile possesses a dominant behavior for (Ag – Fe₃O₄/H₂O) hybrid nanofluid.
- The concentration profile demonstrates a decreasing behavior, with increasing modified Hartman number \mathcal{M}_p and nanoparticle volume fraction.
- The increment in chemical reaction parameter c_R and Schmidt number Sc depicts a clear decline in the concentration profile.
- Skin friction coefficient for (Ag – Fe₃O₄/H₂O) hybrid nanofluid displays an increasing behavior, in the region adjacent to the lower Riga plate, against the varying squeezing parameter γ , modified Hartman number \mathcal{M}_p and the nanoparticle concentration.
- The local heat transfer rate, for (Ag – Fe₃O₄/H₂O) hybrid nanofluid, shows its proficiency for varying nanoparticle concentration, radiation parameter Rd and temperature difference parameter θ_c and this phenomena has been detected at both the plates.
- The augmentation of Schmidt number Sc and chemical reaction parameter c_R enhances the Sherwood number, at the lower plate, while a reversed phenomenon has been observed at the upper plate.

References

1. Choi, S.U.S. Enhancing thermal conductivity of fluids with nanoparticles. In *Developments and Applications of Non-Newtonian Flows*; Siginer, D.A., Wang, H.P., Eds.; ASME: New York, NY, USA, 1995; FED-vol. 231/MD-vol. 66, pp. 99–105.
2. Choi, S.U.S.; Zhang, Z.G.; Yu, W.; Lockwood, F.E.; Grulke, E.A. Anomalous thermal conductivity enhancement in nanotube suspensions. *Appl. Phys. Lett.* **2001**, *79*, 2252–2254, doi:10.1063/1.1408272.
3. Maxwell, J.C. *A Treatise on Electricity and Magnetism*, 3rd ed.; Clarendon; Oxford University Press: Oxford, UK, 1904.
4. Bruggeman, D.A.G. Berechnung der effektiven physikalischen Konstanten von heterogenen Verbänden. *Ann. Phys.* **1935**, *416*, 636–664, doi:10.1002/andp.19354160705.
5. Hamilton, R.L.; Crosser, O.K. Thermal conductivity of heterogeneous two-component systems. *Ind. Eng. Chem. Fundam.* **1962**, *1*, 187–191, doi:10.1021/i160003a005.

6. Suzuki, A.; Ho, N.F.H.; Higuchi, W.I. Predictions of the particle size distribution changes in emulsions and suspensions by digital computation. *J. Colloid Interface Sci.* **1969**, *29*, 552–564, doi:10.1016/0021-9797(69)90140-4.
7. Buongiorno, J. Convective transport in nanofluids. *J. Heat Transf.* **2006**, *128*, 240–250, doi:10.1115/1.2150834.
8. Xue, Q.Z. Model for thermal conductivity of carbon nanotube-based composites. *Phys. B Condens. Matter.* **2005**, *368*, 302–307, doi:10.1016/j.physb.2005.07.024.
9. Iijima, S. Helical microtubules of graphitic carbon. *Nature* **1991**, *354*, 56–58, doi:10.1038/354056a0.
10. Timofeeva, E.V.; Gavrilov, A.N.; McCloskey, J.M.; Tolmachev, Y.V.; Sprunt, S.; Lopatina, L.M.; Selinger, J.V. Thermal conductivity and particle agglomeration in alumina nanofluids: Experiment and theory. *Phys. Rev. E* **2007**, *76*, 061203, doi:10.1103/PhysRevE.76.061203.
11. Masoumi, N.; Sohrabi, N.; Behzadmehr, A. A new model for calculating the effective viscosity of nanofluids. *J. Phys. D Appl. Phys.* **2009**, *42*, 055501, doi:10.1088/0022-3727/42/5/055501.
12. Thurgood, P.; Baratchi, S.; Szydzik, C.; Mitchell, A.; Khoshmanesh, K. Porous PDMS structures for the storage and release of aqueous solutions into fluidic environments. *Lab Chip* **2017**, *17*, 2517–2527, doi:10.1039/C7LC00350A.
13. Sarkar, J.; Ghosh, P.; Adil, A. A review on hybrid nanofluids: Recent research, development and applications. *Renew. Sustain. Energy Rev.* **2015**, *43*, 164–177, doi:10.1016/j.rser.2014.11.023.
14. Ranga Babu, J.A.; Kumar, K.K.; Srinivasa Rao, S. State-of-art review on hybrid nanofluids. *Renew. Sustain. Energy Rev.* **2017**, *77*, 551–565, doi:10.1016/j.rser.2017.04.040.
15. Niihara, K. New Design Concept of Structural Ceramics. *J. Ceram. Soc. Jpn.* **1991**, *99*, 974–982, doi:10.2109/jcersj.99.974.
16. Jana, S.; Salehi-Khojin, A.; Zhong, W.H. Enhancement of fluid thermal conductivity by the addition of single and hybrid nano-additives. *Thermochim. Acta* **2007**, *462*, 45–55, doi:10.1016/j.tca.2007.06.009.
17. Suresh, S.; Venkitaraj, K.P.; Selvakumar, P.; Chandrasekar, M. Synthesis of Al₂O₃-Cu/water hybrid nanofluids using two step method and its thermo physical properties. *Colloids Surf. A Physicochem. Eng. Asp.* **2011**, *388*, 41–48, doi:10.1016/j.colsurfa.2011.08.005.
18. Suresh, S.; Venkitaraj, K.P.; Selvakumar, P.; Chandrasekar, M. Effect of Al₂O₃-Cu/water hybrid nanofluid in heat transfer. *Exp. Therm. Fluid Sci.* **2012**, *38*, 54–60, doi:10.1016/j.expthermflusci.2011.11.007.
19. Momin, G.G. Experimental investigation of mixed convection with water-Al₂O₃ & hybrid nanofluid in inclined tube for laminar flow. *Int. J. Sci. Technol. Res.* **2013**, *2*, 195–202. Devi, S.P.A.; Devi, S.S.U. Numerical investigation of hydromagnetic hybrid Cu-Al₂O₃/water nanofluid flow over a permeable stretching sheet with suction. *Int. J. Nonlinear Sci. Numer.* **2016**, *17*, 249–257, doi:10.1515/ijnsns-2016-0037.
20. Das, S.; Jana, R.N.; Makinde, O.D. MHD Flow of Cu-Al₂O₃/Water Hybrid Nanofluid in Porous Channel: Analysis of Entropy Generation. *Defect Diffus. Forum* **2017**, *377*, 42–61, doi:10.4028/www.scientific.net/DDF.377.42.
21. Chamkha, A.J.; Miroshnichenko, I.V.; Sheremet, M.A. Numerical analysis of unsteady conjugate natural convection of hybrid water-based nanofluid in a semi-circular cavity. *J. Therm. Sci. Eng. Appl.* **2017**, *9*, 1–9, doi:10.1115/1.4036203.
22. Olatundun, A.T.; Makinde, O.D. Analysis of Blasius flow of hybrid nanofluids over a convectively heated surface. *Defect Diffus. Forum* **2017**, *377*, 29–41, doi:10.4028/www.scientific.net/DDF.377.29.
23. Hayat, T.; Nadeem, S. Heat transfer enhancement with Ag-CuO/water hybrid nanofluid. *Results Phys.* **2017**, *7*, 2317–2324, doi:10.1016/j.rinp.2017.06.034.
24. Stefan, M.J. Versuch Uber Die Scheinbare Adhasion, sitzungsber. *Abt.II, Osterr.Akad.Wiss., MathNaturwiss.kl.* **1874**, *69*, 713–721.
25. Shahmohamadi, H.; Rashidi, M.M.; Dinarvand, S. Analytic approximate solutions for unsteady two- dimensional and axisymmetric squeezing flows between parallel plates. *Math. Probl. Eng.* **2008**, *2008*, 1–13, doi:10.1155/2008/935095.
26. Sheikholeslami, M.; Ganji, D.D.; Ashorynejad, H.R. Investigation of squeezing unsteady nanofluid flow using ADM. *Powder Technol.* **2013**, *239*, 259–265, doi:10.1016/j.powtec.2013.02.006.
27. Khan, U.; Ahmed, N.; Asadullah, M.; Mohyud-Din, S.T. Effects of viscous dissipation and slip velocity on two-dimensional and axisymmetric squeezing flow of Cu-water and Cu-kerosene nanofluids. *Propul. Power Res.* **2015**, *4*, 40–49, doi:10.1016/j.jprr.2015.02.004.
28. Ahmed, N.; Khan, U.; Khan, S.I.; Bano, S. Mohyud-Din, S.T. Effects on magnetic field in squeezing flow of a Casson fluid between parallel plates. *J. King Saud Univ. Sci.* **2017**, *29*, 119–125, doi:10.1016/j.jksus.2015.03.006.
29. Gailitis, A.; Lielausis, O. On a possibility to reduce the hydrodynamic resistance of a plate in an electrolyte. *Appl. Magnetohydrodyn.* **1961**, *12*, 143–146.
30. Avilov, V.V. *Electric and Magnetic Fields for the Riga Plate*; Technical Report; FRZ: Rossendorf, Germany, 1998.
31. Pantokratoras, A.; Magyari, E. EMHD free-convection boundary-layer flow from a Riga-plate. *J. Eng. Math.* **2009**, *64*, 303–315, doi:10.1007/s10665-008-9259-6.
32. Pantokratoras, A. The Blasius and Sakiadis flow along a Riga-plate. *Prog. Comput. Fluid Dyn. Int. J.* **2011**, *11*, 329–333, doi:10.1504/PCFD.2011.042184.
33. Magyari, E.; Pantokratoras, A. Aiding and opposing mixed convection flows over the Riga-plate. *Commun. Nonlinear Sci. Numer. Simul.* **2011**, *16*, 3158–3167, doi:10.1016/j.cnsns.2010.12.003.
34. Ayub, M.; Abbas, T.; Bhatti, M.M. Inspiration of slip effects on electromagnetohydrodynamics (EMHD) nanofluid flow through a horizontal Riga plate. *Eur. Phys. J. Plus* **2016**, *131*, 193, doi:10.1140/epjp/i2016-16193-4.
35. Hayat, T.; Khan, M.; Imtiaz, M.; Alsaedi, A. Squeezing flow past a Riga plate with chemical reaction and convective conditions. *J. Mol. Liq.* **2017**, *225*, 569–576, doi:10.1016/j.molliq.2016.11.089.
36. Hayat, T.; Khan, M.; Khan, M.I.; Alsaedi, A.; Ayub, M. Electromagneto squeezing rotational flow of Carbon (C)-Water (H₂O)

- kerosene oil nanofluid past a Riga plate: A numerical study. *PLoS ONE* **2017**, *12*, e0180976, doi:10.1371/journal.pone.0180976.
37. Rosseland, S. *Astrophysik und Atom-Theoretische Grundlagen*; Springer-Verlag: Berlin, Germany, 1931.
 38. Magyari, E.; Pantokratoras, A. Note on the effect of thermal radiation in the linearized Rosseland approximation on the heat transfer characteristics of various boundary layer flows. *Int. J. Heat Mass Transf.* **2011**, *38*, 554–556, doi:10.1016/j.icheatmasstransfer.2011.03.006.
 39. Rashidi, M.M.; Mohimaniyan pour, S.A.; Abbasbandy, S. Analytic approximate solutions for heat transfer of a micropolar fluid through a porous medium with radiation. *Commun. Nonlinear Sci. Numer. Simul.* **2011**, *16*, 1874–1889, doi:10.1016/j.cnsns.2010.08.016.
 40. Noor, N.F.M.; Abbasbandy, S.; Hashim, I. Heat and mass transfer of thermophoretic MHD flow over an inclined radiate isothermal permeable surface in the presence of heat source/sink. *Int. J. Heat Mass Transf.* **2012**, *55*, 2122–2128, doi:10.1016/j.ijheatmasstransfer.2011.12.015.
 41. Mohyud-Din, S.T.; Khan, S.I. Nonlinear radiation effects on squeezing flow of a Casson fluid between parallel disks. *Aerosp. Sci. Technol.* **2016**, *48*, 186–192, doi:10.1016/j.ast.2015.10.019.
 42. Khan, U.; Ahmed, N.; Mohyud-Din, S.T.; Bin-Mohsin, B. Nonlinear radiation effects on MHD flow of nanofluid over a nonlinearly stretching/shrinking wedge. *Neural Comput. Appl.* **2017**, *28*, 2041–2050, doi:10.1007/s00521-016-2187-x.
 43. Saba, F.; Ahmed, N.; Hussain, S.; Khan, U.; Mohyud-Din, S.T.; Darus, M. Thermal Analysis of Nanofluid Flow over a Curved Stretching Surface Suspended by Carbon Nanotubes with Internal Heat Generation. *Appl. Sci.* **2018**, *8*, 395, doi:10.3390/app8030395.
 44. Brinkman, H.C. The viscosity of concentrated suspensions and solutions. *J. Chem. Phys.* **1952**, *20*, 571, doi:10.1063/1.1700493.
 45. Pak, B.C.; Cho, Y.I. Hydrodynamic and heat transfer study of dispersed fluids with submicron metallic oxide particles. *Exp. Heat Transf.* **1998**, *11*, 151–170, doi:10.1080/08916159808946559.
 46. Xuan, Y.; Roetzel, W. Conceptions for heat transfer correlation of nanofluids. *Int. J. Heat Mass Transf.* **2000**, *43*, 3701–3707, doi:10.1016/S0017-9310(99)00369-5.
 47. Ho, C.J.; Huang, J.B.; Tsai, P.S.; Yang, Y.M. Preparation and properties of hybrid water-based suspension of Al₂O₃ nanoparticles and MEPCM particles as functional forced convection fluid. *Int. J. Heat Mass Transf.* **2010**, *37*, 490–494, doi:10.1016/j.icheatmasstransfer.2009.12.007.
 48. Mamut, E. Characterization of heat and mass transfer properties of nanofluids. *Rom. J. Phys.* **2006**, *51*, 5–12.
 49. Singh, P.; Kumar, M. Mass transfer in MHD flow of alumina water nanofluid over a flat plate under slip conditions. *Alexandria Eng. J.* **2015**, *54*, 383–387, doi:10.1016/j.aej.2015.04.005.
 50. Reddy, N.; Murugesan, K. Numerical Investigations on the Advantage of Nanofluids under DDMC in a Lid-Driven Cavity. *Heat Tran. Asian Res.* **2017**, *46*, 1065–1086, doi:10.1002/hjt.21260.
 51. Bergman, T.L.; Lavine, A.S.; Incropera, F.P.; Dewitt, D.P. *Fundamentals of Heat and Mass Transfer*, 4th ed.; John Wiley & Sons: New York, NY, USA, 2002.
 52. Sheikholeslami, M.; Ganji, D.D. Free convection of Fe₃O₄-water nanofluid under the influence of an external magnetic source. *J. Mol. Liq.* **2017**, *229*, 530–540, doi:10.1016/j.molliq.2016.12.101.